ELSEVIER

Ocean Modelling 2 (2000) 45–60

Ocean Modelling

www.elsevier.com/locate/omodol

A numerically efficient data analysis method with error map generation

M. Rixen [a,*], J.M. Beckers [a,1], J.-M. Brankart [b], P. Brasseur [b]

[a] GHER, Institut de Physique, University of Liège, Sart-Tilman B5, B-4000 Liège, Belgium
[b] LEGI, UMR 5519 du CNRS, BP53X, F-38041 Grenoble cedex, France

Abstract

The variational inverse model (VIM) for data analysis was already shown to be statistically equivalent to objective analysis (OA) provided the covariance function for OA and the VIM reproducing kernel are identical. The VIM, however does not allow a direct derivation of the error field associated with the analysis. The purpose of the paper is to extend the one-to-one correspondence between the two analysis schemes by proposing a heuristic statistical error expression for the VIM. The numerical efficiency on analysis and error map generation of both methods is compared on quasi-synoptic and climatological data sets. It is shown that the VIM analysis and error map generation offers interesting numerical skills in both case studies.

Keywords: Objective analysis; Error maps; Variational inverse model; Numerical efficiency

1. Introduction

Among the variety of mapping methods used in geophysical sciences, objective analysis (OA) (sometimes referred to as optimal interpolation) (e.g. Gandin, 1965; Bretherton et al., 1976) and spline interpolation (e.g. Wahba and Wendelberger, 1980; McIntosh, 1990; Brasseur et al., 1996; Brankart and Brasseur, 1996) have become very popular in the last decades for the interpolation of atmospheric and oceanographic observations (e.g. Brasseur et al., 1996). It has already been demonstrated (Kimeldorf and Wahba, 1970; McIntosh, 1990; Bennet, 1992; Brasseur et al., 1996) that there is a statistical equivalence between spline and OA, provided the covariance function for OA and reproducing kernel for norm splines are identical (see Table 1 and details in Appendices A

* Corresponding author. Tel.: +32-4-3663650; fax: +32-4-3662355.
E-mail address: m.rixen@ulg.ac.be (M. Rixen).
[1] Research Associate, National Fund for Scientific Research, Belgium.

1463-5003/00/$ - see front matter
PII: S1463-5003(00)00009-3

Table 1
Statistical equivalence between OA and VIM

	OA	VIM
Minimisation	$e^2(\boldsymbol{x}) = \overline{[\varphi(\boldsymbol{x}) - \varphi_t(\boldsymbol{x})]^2}$	$J[\varphi] \equiv \sum_{i=1}^{N_d} \mu_i [d_i - \varphi(\boldsymbol{x_i})]^2 + \|\varphi\|^2$
Solution	$\varphi(\boldsymbol{x}) = \boldsymbol{c}^{\mathrm{T}}(\boldsymbol{x})\boldsymbol{D}^{-1}\boldsymbol{d}$	$\varphi(\boldsymbol{x}) = \boldsymbol{c}^{\mathrm{T}}(\boldsymbol{x})\boldsymbol{D}^{-1}\boldsymbol{d}$
Data correlation	$[\boldsymbol{D}]_{ij} = c(\boldsymbol{x_i}, \boldsymbol{x_j}) + \sigma^2(\boldsymbol{x_i})\delta_{ij}$	$[\boldsymbol{D}]_{ij} = K(\boldsymbol{x_i}, \boldsymbol{x_j}) + (1/\mu)\delta_{ij}$
Data-field covariance	$[\boldsymbol{c}]_i = c(\boldsymbol{x}, \boldsymbol{x_i})$	$[\boldsymbol{c}]_i = K(\boldsymbol{x}, \boldsymbol{x_i})$

and B). Numerous improvements of the classical analysis schemes have been proposed in order to work with different data types and to improve the numerical efficiency and the quality of the analysed field (e.g. Brankart and Brasseur, 1996; Menemenlis et al., 1997). As discussed in Sokolov and Rintoul (1999), each method has certain advantages compare to the others, depending on the amount of data, the analysis grid, the accuracy of the analysis, the knowledge of the correlation function, the presence of islands, ...

OA is based on the minimisation of a statistical error estimation and allows the simultaneous derivation of the analysis and the error field. The numerical cost may however become prohibitive for large data sets. On the contrary, smoothing spline interpolation, based on the minimisation of a variational principle solved by a finite-element technique (e.g. Brasseur et al., 1996) is very efficient for large data sets, but the formulation does not offer a direct statistical error estimation.

The purpose of the paper is to study a heuristic formulation of the statistical error of the variational inverse model (VIM), derived from the one-to-one correspondence between OA and VIM (Section 2). The numerical efficiency of the schemes is compared (Section 3). Test experiments are then conducted on two very different observation data sets (Section 4) in order to further examine the practical properties of the two methods. Both analysis schemes are summarised in Appendices A and B.

2. Error estimation

The OA analysis scheme is based on the minimisation of a statistical error estimation. It is assumed that the field to estimate is one realisation out of a zero mean ensemble. Noting $\boldsymbol{d} = (d_1 \ldots d_{N_d})$ the observation vector and $\varphi(\boldsymbol{x})$ the analysed field at location $\boldsymbol{x}$, the solution reads

$$\varphi(\boldsymbol{x}) = \boldsymbol{c}^{\mathrm{T}}(\boldsymbol{x})\boldsymbol{D}^{-1}\boldsymbol{d}, \tag{1}$$

where $\boldsymbol{D}$ is the observation covariance matrix and $\boldsymbol{c}(\boldsymbol{x})$ is the vector of prior error covariances between each observation point and the location $\boldsymbol{x}$ (see Appendix A for details).

The OA allows a straightforward derivation of the expected error variance $e^2(\boldsymbol{x})$ associated with the solution

$$e^2(\boldsymbol{x}) = \epsilon^2(\boldsymbol{x}) - \boldsymbol{c}^{\mathrm{T}}(\boldsymbol{x})\boldsymbol{D}^{-1}\boldsymbol{c}(\boldsymbol{x}), \tag{2}$$

where $\epsilon^2(\boldsymbol{x})$ is the prior error variance. Eqs. (1) and (2) imply that the error variance on the solution is the prior error variance diminished by an analysis of the $\boldsymbol{c}(\boldsymbol{x})$ vector. In areas void of data, $e \sim \epsilon$. In areas full of data, the error can be strongly reduced.

On the other hand, by solving the VIM with a finite element technique, the solution reads (see Appendix B for details)

$$\varphi(\boldsymbol{x}) = \boldsymbol{T_1}(\boldsymbol{x})\boldsymbol{K}^{-1}\boldsymbol{T_2}(\boldsymbol{x})\boldsymbol{d}, \tag{3}$$

where $\boldsymbol{T_1}$ and $\boldsymbol{T_2}$ are two transfer operators and $\boldsymbol{K}$ is the stiffness matrix of the problem.

The VIM formulation however does not offer an estimation of the error on the analysis, but the analogy between solutions (1) and (3) suggests to compute directly

$$e^2(\boldsymbol{x}) = \epsilon^2(\boldsymbol{x}) - \boldsymbol{T_1}(\boldsymbol{x})\boldsymbol{K}^{-1}\boldsymbol{T_2}(\boldsymbol{x})\boldsymbol{c}(\boldsymbol{x}) \tag{4}$$

assuming $\boldsymbol{c}^{\mathrm{T}}(\boldsymbol{x})\boldsymbol{D}^{-1} \sim \boldsymbol{T_1}(\boldsymbol{x})\boldsymbol{K}^{-1}\boldsymbol{T_2}(\boldsymbol{x})$.

An estimation of the statistical error is thus obtained by analysing the $\boldsymbol{c}(\boldsymbol{x})$ vector field at each location $\boldsymbol{x}$. The $\boldsymbol{K}$ matrix was already used for the analysis (Eq. (3)) and does not need to be reconstructed again to compute $e^2(\boldsymbol{x})$.

This method is an hybridation of the objective scheme and the variational scheme. Indeed, whilst the correlation function is hidden in the VIM analysis, it has to be explicitly computed at each location $\boldsymbol{x}$ in order to derive the statistical error. So, the correlation function appears twice in the error estimation, in the variational principle, where is it hidden, and explicitly like in usual optimal interpolation.

It is not proved that this technique is statistically fully consistent, but it should be obvious that near the boundaries, this solution will not suffer from the biases inherent to the OA. Indeed, without taking into account the natural boundaries, i.e. with a homogeneous and isotropic statistical model, the solution will be attracted towards the background field in areas void of data and the error standard deviation e towards the background error standard deviation ϵ. Indeed, the latter overestimates the error and biases the solution in coastal areas and near islands (Brankart and Brasseur, 1998), whereas the VIM method takes into account the geometry of the system and prevents information to cross land barriers. The main advantage of the VIM is thus to adapt automatically the statistical model by decorrelating the links between land and sea. A rigorous dissection of Eq. (4) seems difficult because the statistics are hidden in the VIM but it is impossible to deny that a sensible improvement is obtained through this assumption compared to standard OA (see Section 3).

3. Numerical efficiency

In this section, we will consider the original OA and VIM analysis schemes, bearing in mind that numerous improvements have been proposed in order to increase the numerical efficiency of both schemes.

Let us define N_e and N_l as the number of elements and degrees of freedom in the finite element mesh, respectively and N_ϕ as the number of grid point where the solution is computed. Usually, $N_l \sim [3\text{–}4]N_e$, depending on the complexity of the domain (islands, coastline, ...).

The number of algebraic operations necessary to produce a gridded field using OA is approximately (Brasseur et al., 1996)

$$C_{\mathrm{OA_A}} = k_1 N_d^3 + k_2 N_d N_\phi, \tag{5}$$

corresponding to Eq. (1). The k_i coefficients are constants.

The first contribution, proportional to N_d^3, corresponds to the LU decomposition, whereas the second term represents the projection of the solution from the 'observational' space onto the domain.

The equivalent number of operations for the VIM necessary to solve Eq. (3) yields (Brasseur et al., 1996)

$$C_{\mathrm{VIM_A}} = k_3 N_l^{5/2} + k_4 N_l N_\phi, \tag{6}$$

independent of the number of observations. The first contribution, proportional to the power 5/2 of the number of degrees of freedom of the finite-element discretisation, represents the numerical cost of the 'stiffness' matrix inversion, if the elements are assembled using the skyline algorithm (Dhatt, 1984). The second term the projection from the 'model' space onto the grid. The cost of the data projection into the model space is negligible.

Similarly, the number of operations involved in the derivation of the statistical error (2) yields

$$C_{\mathrm{OA_E}} = k_1 N_d^3 + k_5 N_d^2 N_\phi, \tag{7}$$

involving the inversion of the 'influence coefficients' (first contribution) and the 'projection' of the $\boldsymbol{c}(\boldsymbol{x})$ vector field at each location $\boldsymbol{x}$ (second contribution).

The corresponding numerical cost of statistical error derivation for the VIM (Eq. (4)) yields

$$C_{\mathrm{VIM_E}} = k_3 N_l^{5/2} + k_6 N_l^2 N_\phi, \tag{8}$$

where the first contribution again corresponds to the stiffness matrix inversion and the second term corresponds to the analysis of the $\boldsymbol{c}(\boldsymbol{x})$ vector field at each location $\boldsymbol{x}$.

Table 2 summarises the order of magnitude of the numerical costs for OA and VIM. The OA requires the computation of the correlation function, whilst it is inherent to the VIM analysis. When deriving the statistical error field for the VIM, the correlation function has however to be computed explicitly.

The computational cost of the inversion of the matrix $\boldsymbol{D}$ for OA is proportional to the cube of the number of data $\mathrm{O}(N_d^3)$, and makes it prohibitive for large data sets such as climatological data bases (line 1). The cost of inversion of the matrix $\boldsymbol{K}$ in the VIM is proportional to the power 5/2 of the degrees of freedom N_l of the finite element mesh, namely $\mathrm{O}(N_l^{5/2})$ (see Appendix B).

Table 2
Comparison of computational cost of OA and VIM (order of magnitude of dominant terms)

	OA	VIM
Matrix inversion	$(1/6)N_d^3$	$N_l^{5/2}$
Analysis (without inversion)	$N_\phi N_d$	$N_\phi N_l$
Statistical error (without inversion)	$N_\phi N_d^2$	$N_\phi N_l^2$

After completion of the inversion, the projection of the solution onto the analysis grid requires $O(N_d N_\phi)$ operations for the OA whilst it is of $O(N_l N_\phi)$ for the VIM (line 2).

The statistical error computation for the OA is of order $O(N_\phi N_d^2)$ and for the VIM, $O(N_\phi N_l^2)$ (last 3).

Generally, we have $N_\phi > \sqrt{N_l}$, so the error computation is usually much more expensive than the analysis itself.

The Nyquist's theory tells us that, in the case of a uniform data spatial distribution, $N_e = O(N_d)$ elements are enough to obtain an analysis with sufficient accuracy. Finer meshes are usually not necessary since the solution for each element is already approximated by a third-order polynomial. Moreover, finer physical scales cannot be resolved by finer meshes following Nyquist's theory.

Considering the dominant terms in the analysis cost (Eqs. (5) and (6)), and excluding the error map generation, one gets a first estimate of the critical number of data N_o over which the VIM becomes numerically cheaper

$$\frac{1}{6}N_d^3 = N_l^{5/2} \sim (4N_e)^{5/2} \sim (4N_d)^{5/2} \tag{9}$$

yielding $N_o = 576$ data. If $N_l \sim 3N_e$, then $N_o = 324$.

The error computation becomes faster as soon as $N_l < N_d$ (for large N_ϕ), that is, when there are at least a few observations per finite element.

In practice, the VIM code is more complicated and the overhead computation cost is greater. Therefore, the choice between OA and VIM will depend upon both the number of data N_d and the number of degrees of freedom N_l involved (and to some extent upon the number of grid points N_ϕ).

4. Examples

In the following examples, the free parameters of the analysis, a signal-to-noise ratio $S/N = \epsilon^2/\sigma^2$ and a characteristic length L have been calibrated by generalised cross validation (Wahba and Wold, 1975; Craven and Wahba, 1979; Golub et al., 1979; Brankart and Brasseur, 1996; Rixen et al., 2001). In the OA, the correlation function can be chosen freely, whereas in the VIM the shape of the correlation function is inherent to the problem formulation (Brasseur et al., 1996; Brankart and Brasseur, 1996). In order to compare both OA and VIM, a common correlation function, namely

$$c(r) = \frac{r}{L}K_1\left(\frac{r}{L}\right), \tag{10}$$

(where K_1 is the modified Bessel function of order 1), has been chosen for our computations. A linear regression of the data provides a common background field for both OI and VIM in order to make the comparison easier. In practice however, it is preferable to use a semi-normed reference field obtained by dropping the underived term in the VIM. This latter procedure reduces unphysical features in the analysis (Brankart and Brasseur, 1996). The finite elements and the grid resolution have been chosen to fit the characteristic length of the physical processes under study. As each element is divided into 3 sub-elements representing a polynomial of order 3, the real characteristic length of each sub-element is even smaller than the element itself (roughly a factor 2).

The benchmarks were run on a node of an IBM/SP2 RISC/6000 computer (160 Mhz).

4.1. *Quasi-synoptic data set*

The first example involves a quasi-synoptic data set (Viúdez et al., 1996) included in the MODB Data Base (Brasseur et al., 1996; Brankart and Brasseur, 1996), originating from a field experiment carried out from 22 September to 7 October 1992 on board the R/V *Garcia del Cid*, resulting in a quasi-regular grid covering the entire Alboran Sea (108 stations), a two basins area located between Spain and Morocco in the Mediterranean Sea. The analysis and statistical error have been computed on a 91×61 grid with a resolution of $0.05^\circ \times 0.05^\circ$ (4.532×5.585 km^2).

The VIM finite element mesh has been constructed with a characteristic length scale of 50 km, contains 172 elements and has 775 degrees of freedom. The statistical parameters $L = 30$ km, $\epsilon = 0.36$ and $\sigma = 0.13$ were optimised by GCV. Fig. 1 shows the salinity at 120 m depth for OA (top) and VIM (middle) and the difference between the two fields (bottom). Main differences between the two solutions are located in coastal areas of the Alboran Sea, but within the domain, discrepancies range between -0.01 and 0.02 only.

Fig. 2 shows the statistical error of the salinity field corresponding to Fig. 1 at 120 m depth for OA (top) and VIM (middle) and the difference between the two fields (bottom). The statistical error for both solution is limited to 0.15. The difference between the two estimators is less than 0.005, except along the boundaries where values of up to 0.09 are found. The proposed heuristic statistical error is thus in good agreement with the OA theory.

Fig. 3 illustrates a comparison of the numerical performances of the OA and VIM schemes (with the same configuration – N_l, N_ϕ) as a function of the number of observations (arbitrary data values). The VIM analysis becomes faster than OA when more than 250 data are available (top figure). The error map generation for the VIM becomes faster when more than 135 data are used (bottom figure).

4.2. *Climatological data set*

The second example involves a selection of the MODB climatological data base at the surface in June, namely 1858 stations (see Fig. 4). We see that the Western Mediterranean Sea is well covered, specially along coastal areas, whereas the Eastern Mediterranean Sea lacks data. The analysis and statistical error have been computed on a 184×63 grid, with a resolution of $0.25^\circ \times 0.25^\circ$ (22.080×27.925 km^2). The VIM finite element mesh has been constructed with a characteristic length scale of 100 km, contains 801 elements and has 3077 degrees of freedom. The statistical parameters obtained by GCV yield respectively, $L = 180$ km, $\epsilon = 0.20$ and $\sigma = 0.23$. Fig. 5 shows the surface analysis of this salinity data set obtained by OA (top), VIM (middle) and the difference between the two analyses (bottom). Conclusions are similar to the previous example. The OA and VIM provide almost identical fields, except in coastal areas and around islands where differences of up to 0.1 are found. The extreme discrepancy found in the Aegean Sea may be explained both by the strong extrapolation occurring there because of lacking data and also by the behaviour of each analysis method. Whilst the OA allows the correlation function to 'cross' land, the VIM prohibits this bias. Fig. 6 shows the statistical error of the OA (top), VIM (middle) and the difference between both fields (bottom). Again, differences are very tiny, except in coastal areas, where values up to 0.1 are found.

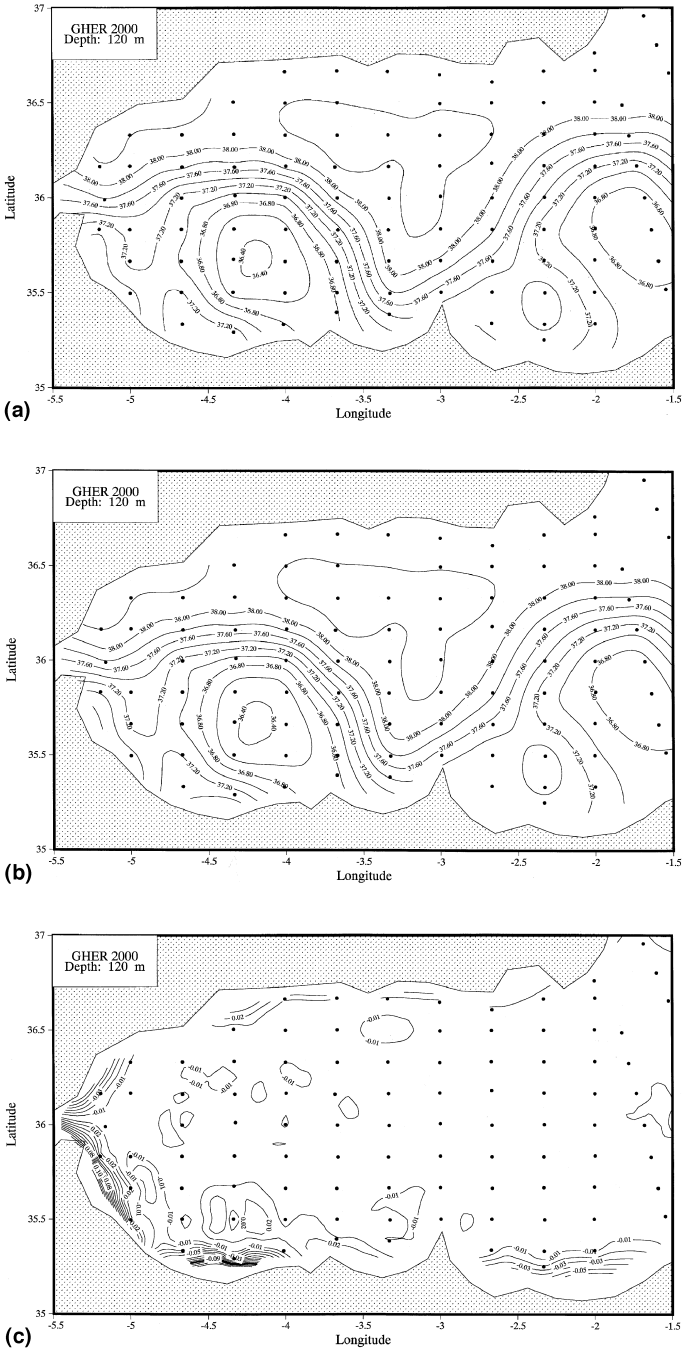

Fig. 1. Example 1: salinity field (91×61 grid points) at 120 m for OA (top, $\Delta = 0.2$), VIM (middle, $\Delta = 0.2$) and difference between the two fields (bottom, $\Delta = 0.01$).

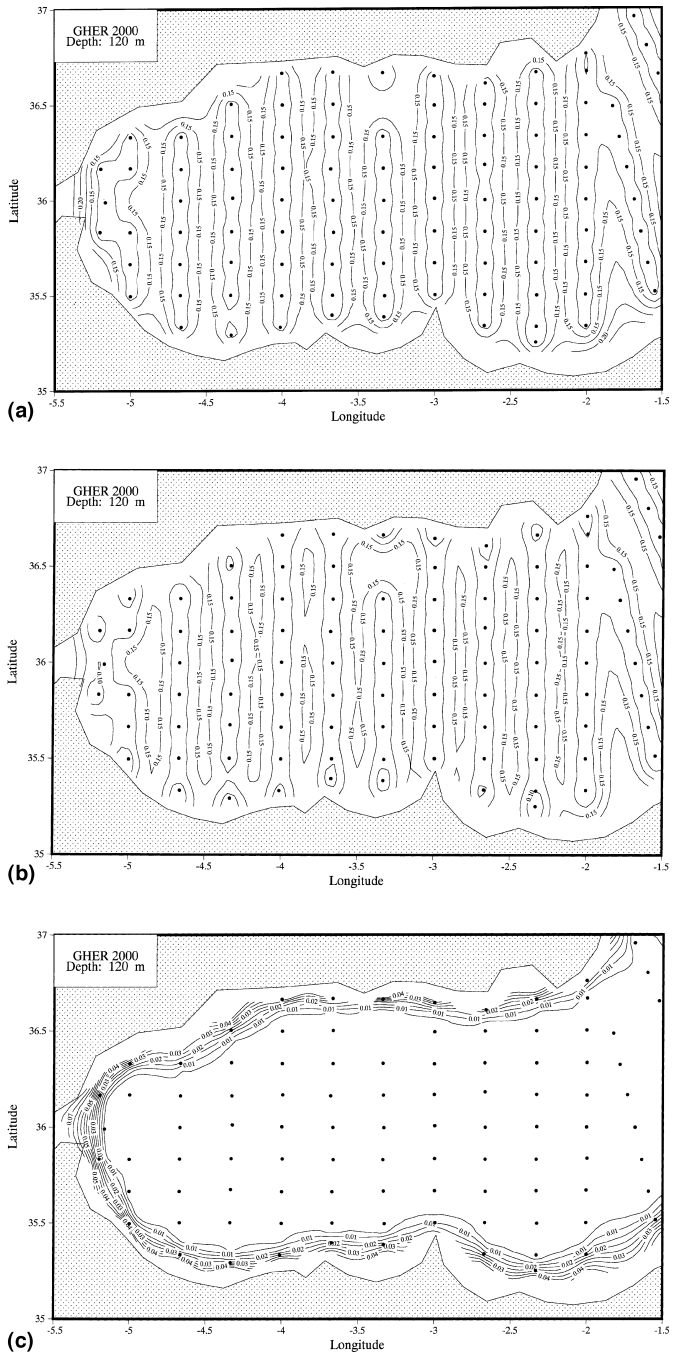

Fig. 2. Example 1: statistical error of salinity field (91 × 61 grid points) at 120 m for OA (top, $\Delta = 0.025$), VIM (middle, $\Delta = 0.025$) and difference between the two fields (bottom, $\Delta = 0.005$).

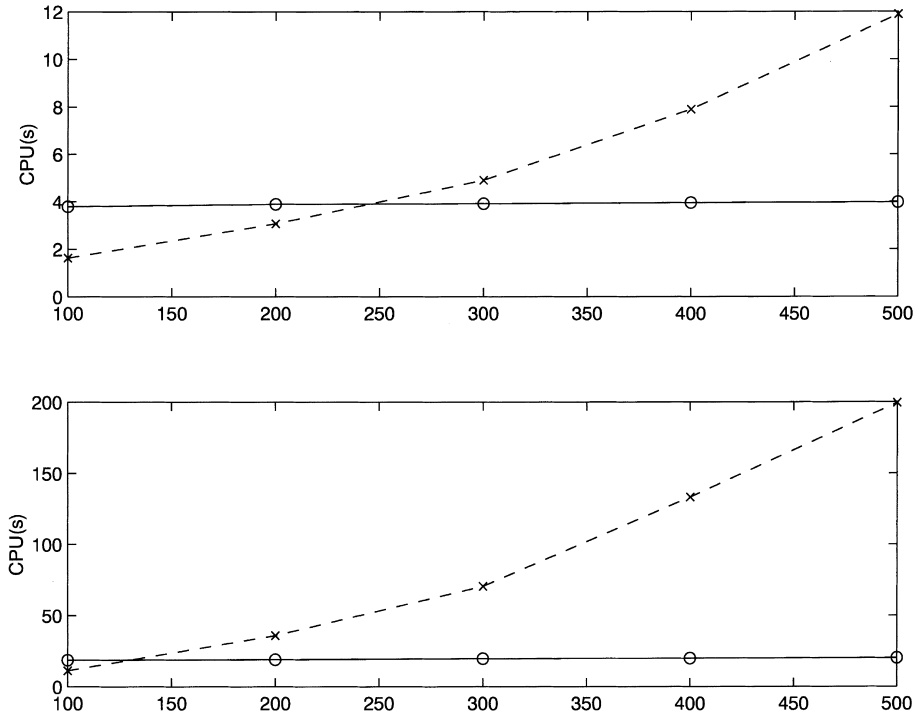

Fig. 3. Example 1: CPU time (s) needed to perform variational (solid line) and objective (dashed line) analysis (top) and error map generation (bottom) as a function of the number of observations.

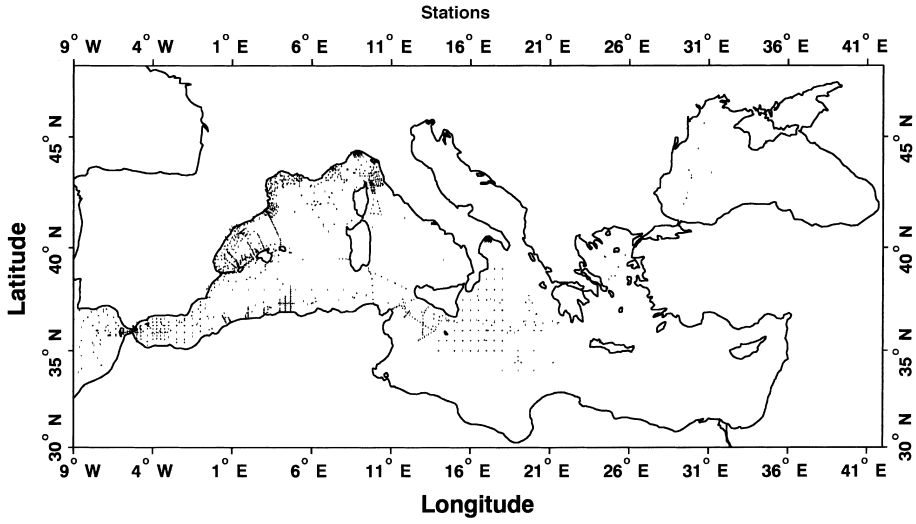

Fig. 4. Example 2: climatological salinity stations in June at the surface.

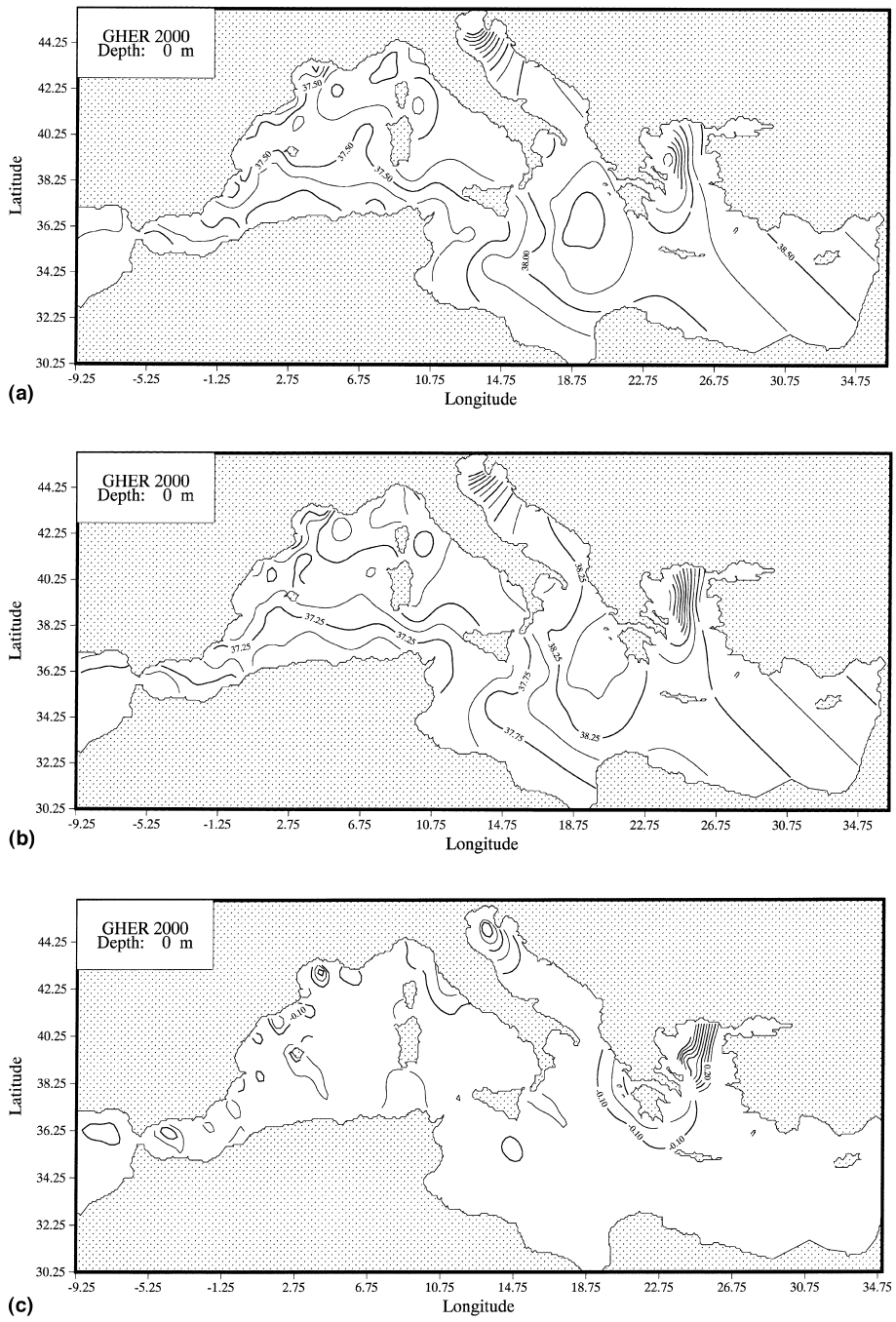

Fig. 5. Example 2: climatological salinity field (184 × 63 grid points) in June at the surface for OA (top, $\Delta = 0.25$), VIM (middle, $\Delta = 0.25$) and difference between the two fields (bottom, $\Delta = 0.1$).

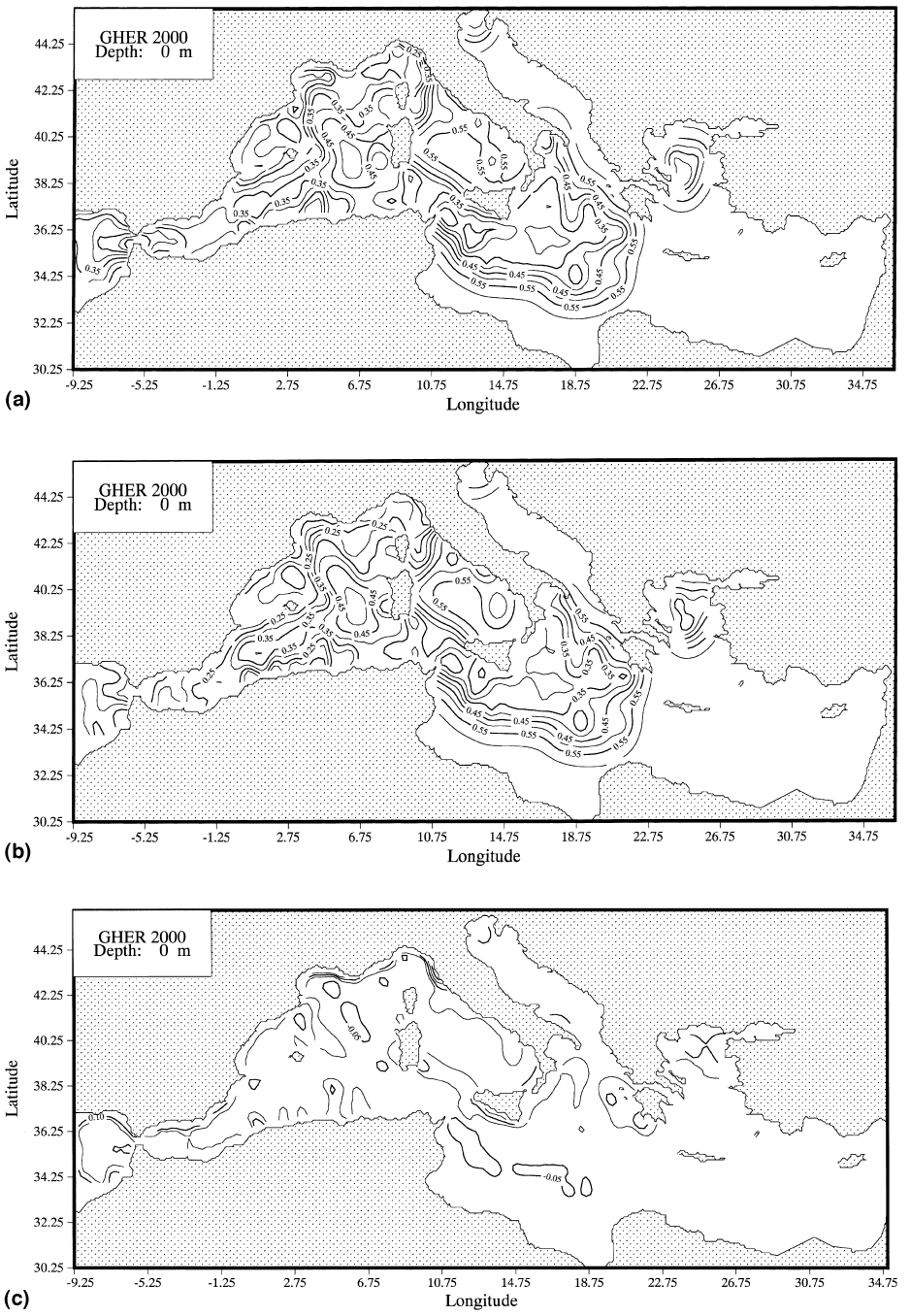

Fig. 6. Example 2: statistical error of climatological salinity field (184 × 63 grid points) in June at the surface for OA (top, $\Delta = 0.05$), VIM (middle, $\Delta = 0.05$) and difference between the two fields (bottom, $\Delta = 0.05$).

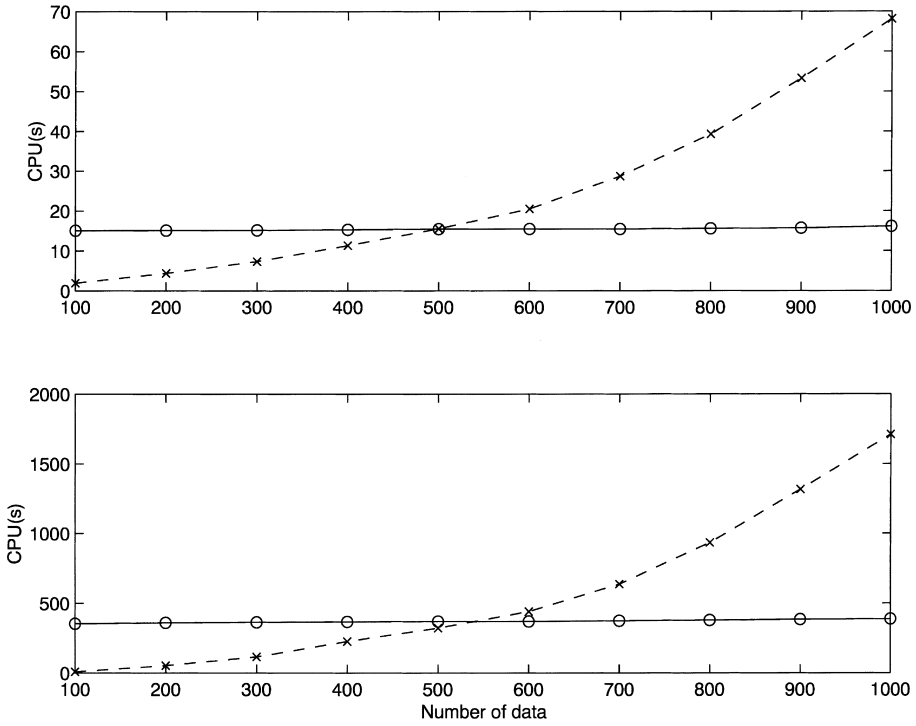

Fig. 7. Example 2: CPU time (s) needed to perform variational (solid line) and objective (dashed line) analysis (top) and error map generation (bottom) as a function of the number of observations.

Similarly to Fig. 3, Fig. 7 illustrates a comparison of the numerical performances of the OA and VIM schemes as a function of the number of observations. The VIM analysis becomes faster than OA when more than 500 data are available (top figure). The error map generation becomes faster for the VIM when more than 550 data are used (bottom figure).

5. Conclusions

A heuristic statistical error estimation has been derived from the statistical analogy between OA and VIM. This estimation has been tested on two distinct test cases and was shown to be consistent with the classical estimation of the OA. The VIM analysis and error map generation (with or without optimised parameters) are attractive for both synoptic and climatological data sets. The variational inverse model (VIM) is the analysis tool of the MODB data base and may be downloaded free of charge at `http://www.modb.oce.ulg.ac.be`.

Acknowledgements

The error map analysis was developed in the scope of MATER contract MAS3-CT96-0051 and MEDAR contract MAS3-CT98-0174 of the European Union.

Appendix A. Optimal interpolation

Optimal interpolation, as developed by Gandin (1965), Bretherton et al. (1976), assumes that the true field $\varphi_t(\boldsymbol{x})$ that we are estimating is one realisation out of a zero mean ensemble. The solution $\varphi(\boldsymbol{x})$ is expressed as a linear combination of the N_d observations d_i at $\boldsymbol{x}_i$

$$\varphi(\boldsymbol{x}) = \sum_{i=1}^{N_d} \eta_i(\boldsymbol{x}) d_i = \boldsymbol{\eta}^{\mathrm{T}}(\boldsymbol{x})\boldsymbol{d}. \tag{A.1}$$

The principle of the method is to minimise the expected error

$$e^2(\boldsymbol{x}) = \overline{[\varphi(\boldsymbol{x}) - \varphi_t(\boldsymbol{x})]^2}. \tag{A.2}$$

Replacing (A.1) in (A.2), one obtains

$$e^2(\boldsymbol{x}) = \overline{\varphi_t^2(\boldsymbol{x})} + \boldsymbol{\eta}^{\mathrm{T}}(\boldsymbol{x})\overline{\boldsymbol{d}\boldsymbol{d}^{\mathrm{T}}}\boldsymbol{\eta}(\boldsymbol{x}) - 2\boldsymbol{\eta}^{\mathrm{T}}(\boldsymbol{x})\overline{\boldsymbol{d}\varphi_t(\boldsymbol{x})}. \tag{A.3}$$

Noting $c(\boldsymbol{x},\boldsymbol{y})$ the prior (or background) covariance and $\epsilon^2(\boldsymbol{x}) = c(\boldsymbol{x},\boldsymbol{x})$ the corresponding variance, it transforms (assuming that observation error and background error are uncorrelated)

$$e^2(\boldsymbol{x}) = \epsilon^2(\boldsymbol{x}) + \boldsymbol{\eta}^{\mathrm{T}}(\boldsymbol{x})\boldsymbol{D}\boldsymbol{\eta}(\boldsymbol{x}) - 2\boldsymbol{\eta}^{\mathrm{T}}(\boldsymbol{x})\boldsymbol{c}(\boldsymbol{x}), \tag{A.4}$$

where $\boldsymbol{D}$ is the observation covariance matrix and $\boldsymbol{c}(\boldsymbol{x})$ is the vector of prior covariance between the observations and analysis locations

$$[\boldsymbol{c}(\boldsymbol{x})]_i = c(\boldsymbol{x},\boldsymbol{x}_i). \tag{A.5}$$

Noting $\sigma^2(\boldsymbol{x})$ the observation error variances, and assuming that the observations are independent, the matrix $\boldsymbol{D}$ writes

$$[\boldsymbol{D}]_{ij} = c(\boldsymbol{x}_i,\boldsymbol{x}_j) + \sigma^2(\boldsymbol{x}_i)\delta_{ij}. \tag{A.6}$$

One verifies that the error given by Eq. (A.4) is minimum everywhere if

$$\boldsymbol{D}\boldsymbol{\eta}(\boldsymbol{x}) = \boldsymbol{c} \tag{A.7}$$

and the optimal solution to the problem thus reads

$$\varphi(\boldsymbol{x}) = \boldsymbol{c}^{\mathrm{T}}(\boldsymbol{x})\boldsymbol{D}^{-1}\boldsymbol{d} \tag{A.8}$$

with the associated minimum expected error

$$e^2(\boldsymbol{x}) = \epsilon^2(\boldsymbol{x}) - \boldsymbol{c}^{\mathrm{T}}(\boldsymbol{x})\boldsymbol{D}^{-1}\boldsymbol{c}(\boldsymbol{x}). \tag{A.9}$$

Defining the transfer operator $\boldsymbol{H}(\boldsymbol{x}) = \boldsymbol{c}^{\mathrm{T}}(\boldsymbol{x})\boldsymbol{D}^{-1}$ the solution reads

$$\varphi(\boldsymbol{x}) = \boldsymbol{H}(\boldsymbol{x})\boldsymbol{d}, \tag{A.10}$$

$$e^2(\boldsymbol{x}) = \epsilon^2(\boldsymbol{x}) - \boldsymbol{H}(\boldsymbol{x})\boldsymbol{c}(\boldsymbol{x}). \tag{A.11}$$

Appendix B. VIM

The VIM provides an elegant solution to the very classical problem of interpolating/analysing a discrete set of N_d dispersed data points d_i at $\boldsymbol{x}_i$. Expressed in mathematical terms, the result of the analysis, i.e. the field φ, is obtained as the minimum of a variational principle on the domain of interest Ω (e.g. Brasseur et al., 1996):

$$\min_{\varphi} J[\varphi], \quad J[\varphi] \equiv \sum_{i=1}^{N_d} \mu_i [d_i - \varphi(\boldsymbol{x}_i)]^2 + \|\varphi\|^2 \tag{B.1}$$

with the norm defined as

$$\|\varphi\|^2 = \int_{\Omega} \left(\alpha_2 \nabla\nabla\varphi : \nabla\nabla\varphi + \alpha_1 \nabla\varphi \cdot \nabla\varphi + \alpha_0 \varphi^2\right) \mathrm{d}\Omega, \tag{B.2}$$

where μ_i is the weight on the data, α_0 the weight on φ, α_1 the weight on the slope of φ, α_2 the weight on the curvature of φ, $\boldsymbol{A} : \boldsymbol{B}$ is the scalar product of two tensors $\boldsymbol{A}$ and $\boldsymbol{B}$.

The first contribution of the variational principle represents the distance between the data d_i at location $\boldsymbol{x}_i$ and the target field φ. The second contribution is a measure of the magnitude, slope and curvature of the target field.

It can be shown that on an infinite domain the solution to the variational problem (B.1) can be written (K is the reproducing kernel of the Hilbert space whose norm is defined by Eq. (B.2) (Brasseur et al., 1996)

$$\varphi(\boldsymbol{x}) = \boldsymbol{c}^{\mathrm{T}}(\boldsymbol{x}) \boldsymbol{D}^{-1} \boldsymbol{d} \tag{B.3}$$

with the data correlation matrix

$$[\boldsymbol{D}]_{ij} = K(\boldsymbol{x_i}, \boldsymbol{x_j}) + \frac{1}{\mu} \delta_{ij} \tag{B.4}$$

and the data-field covariance

$$c_i(\boldsymbol{x}) = K(\boldsymbol{x}, \boldsymbol{x_i}). \tag{B.5}$$

The Eqs. (B.3), (B.4) and (B.5) correspond respectively, to the OA equations (A.5), (A.6) and (A.8), thus one writes $\mu = 1/\sigma^2$.

Obviously, the VIM may be solved by Eqs. (B.3), (B.4) and (B.5), but the numerical cost is then equivalent to the OA.

This problem may be circumvented by solving the minimisation problem (B.1) with a finite element technique. The arbitrary real geometry is then split in a mesh of N_e finite elements and the global variational principle is expressed as the sum of elementary functions

$$J(\varphi) = \sum_{e=1}^{N_e} J_e(\varphi_e). \tag{B.6}$$

The solution is then approximated on each element by a linear combination of a known set of shape functions $\boldsymbol{s}$ (a polynomial base of order 3) and the continuity of the solution is guaranteed by identification of adjacent connectors:

$$\varphi_e(\boldsymbol{x}_e) = \boldsymbol{q}_e^{\mathrm{T}} \boldsymbol{s}(\boldsymbol{x}_e), \tag{B.7}$$

where $\boldsymbol{x}_e$ is the position in a local coordinate system, and $\boldsymbol{q}_e$ is the vector of connectors.

The elementary problem then reads

$$J_e(\boldsymbol{q}_e) = \boldsymbol{q}_e^{\mathrm{T}} \boldsymbol{K}_e \boldsymbol{q}_e - 2\boldsymbol{q}_e^{\mathrm{T}} \boldsymbol{g}_e + \sum_{i=1}^{N_{de}} \mu_i d_i^2, \tag{B.8}$$

where $\boldsymbol{K}_e$ is the local stiffness matrix and $\boldsymbol{g}$ depends on the local data.

The global variational principle may then be written as (Brasseur et al., 1996)

$$J(\boldsymbol{q}) = \boldsymbol{q}^{\mathrm{T}} \boldsymbol{K} \boldsymbol{q} - 2\boldsymbol{q}^{\mathrm{T}} \boldsymbol{g} + \sum_{i=1}^{N_d} \mu_i d_i^2, \tag{B.9}$$

where $\boldsymbol{K}$ is the stiffness matrix and $\boldsymbol{g}$ depends on the data.

This expression is minimum when

$$\boldsymbol{q} = \boldsymbol{K}^{-1} \boldsymbol{g}. \tag{B.10}$$

The size of the matrix $\boldsymbol{K}$ is proportional to the number of degrees of freedom of the system. If the elements are correctly sorted, then the resulting matrix is therefore very sparse and leads to a computational cost roughly proportional to the power 5/2 of the number of degrees of freedom. Consequently, the major part of the computation does not depend on the size of the data set.

The data are mapped on the finite element mesh through a transfer operator $\boldsymbol{T}_2$

$$\boldsymbol{g} = \boldsymbol{T}_2(\boldsymbol{x}) \boldsymbol{d}. \tag{B.11}$$

As the solution is naturally continuous, the result may be computed everywhere inside the domain through a second transfer operator $\boldsymbol{T}_1$

$$\varphi(\boldsymbol{x}) = \boldsymbol{T}_1(\boldsymbol{x}) \boldsymbol{q}. \tag{B.12}$$

Consequently, the result may be extracted at any location

$$\varphi(\boldsymbol{x}) = \boldsymbol{T}_1 \boldsymbol{K}^{-1} \boldsymbol{T}_2 \boldsymbol{d}. \tag{B.13}$$

References

Bennet, A., 1992. Inverse methods in physical oceanography. Cambridge Monographs on Mechanics and Applied Mathematics. Cambridge University Press.

Brankart, J.-M., Brasseur, P., 1996. Optimal analysis of in situ data in the Western Mediterranean using statistics and cross-validation. Journal of Atmospheric and Oceanic Technology 13 (2), 477–491.

Brankart, J.-M., Brasseur, P., 1998. The general circulation in the Mediterranean Sea: a climatological approach. Journal of Marine Systems 18, 41–70.

Brasseur, P., Beckers, J.-M., Brankart, J.-M., Schoenauen, R., 1996. Seasonal temperature and salinity fields in the Mediterranean Sea: climatological analyses of an historical data set. Deep-Sea Research 43 (2), 159–192.

Bretherton, F.P., Davis, R.E., Fandry, C.B., 1976. A technique for objective analysis and design of oceanographic experiment applied to MODE-73. Deep-Sea Research 23, 559–582.

Craven, P., Wahba, G., 1979. Smoothing noisy data with spline functions: estimating the correct degree of smoothing by the method of generalized cross-validation. Numerical Mathematics 31, 377–403.

Dhatt, G.A., 1984. Une présentation de la méthode des éléments finis. In: Maloine, S.A. (Ed.), Collection Université de Compiégne, Paris.

Gandin, L.S., 1965. Objective analysis of meteorological fields. Israel Program for Scientific Translation, Jerusalem, pp. 242.

Golub, G.H., Heath, M., Wahba, G., 1979. Generalized cross-validation as a method for choosing a good ridge parameter. Technometrics 21 (2), 215–223.

Kimeldorf, G., Wahba, G., 1970. A correspondence between Bayesian estimation of stochastic processes and smooting by splines. Annals of Mathematical Statistics 41, 495–502.

McIntosh, P., 1990. Oceanographic data interpolation: objective analysis and spline. Journal of Geophysical Research 95 (C8), 13529–13541.

Menemenlis, D., Fieguth, P., Wunsch, C., Willsky, A., 1997. Adaptation of a fast optimal interpolation algorithm to the mapping of oceanographic data. Journal of Geophysical Research 102 (C5), 10573–10584.

Rixen, M., Allen, J., Beckers, J.-M., 2001. Non-synoptic versus pseudo-synoptic data sets: an assimilation experiment. In: Three-dimensional ocean circulation: Lagrangian measurements and diagnostic. Journal of Marine Systems (in press).

Sokolov, S., Rintoul, S., 1999. Some remarks on interpolation of non-stationary oceanographic fields. Journal of Atmospheric and Oceanic Technology 16, 1434–1449.

Viúdez, A., Tintoré, J., Haney, R., 1996. Circulation in the Alboran Sea as determined by quasi-synoptic hydrographic observations. Part I: three-dimensional structure of the two anticyclonic gyres. Journal of Physical Oceanography 26, 684–705.

Wahba, G., Wendelberger, J., 1980. Some new mathematical methods for variational objective analysis using splines and cross validation. Monthly Weather Review 108, 1122–1143.

Wahba, G., Wold, S., 1975. A completely automatic French curve. Communications in Statistics 4, 1–17.